frontiers in Materials

ORIGINAL RESEARCH
published: 09 March 2022
doi: 10.3389/fmats.2022.845349

A Comparative Study on the Degradation of Alkali-Activated Slag/Fly Ash and Cement-Based Mortars in Phosphoric Acid

Jie Ren[1,2], *Lihai Zhang*[1], *Yingcan Zhu*[3]*, *Zhenming Li*[4]* and *Rackel San Nicolas*[1]

[1]Department of Infrastructure Engineering, the University of Melbourne, Parkville, VIC, Australia, [2]Department of Civil, Environment, and Architectural Engineering, University of Colorado Boulder, Boulder, CO, United States, [3]Centre for Sustainable Agricultural Systems, University of Southern Queensland, Toowoomba, QLD, Australia, [4]Department of Materials and Environment, Faculty of Civil Engineering and Geoscience, Delft University of Technology, Delft, Netherlands

This study compares the degradation behavior of the alkali-activated slag/fly ash (AASF) and ordinary Portland cement (OPC) mortars exposed to phosphoric acid with different pH values. The experimental results show that AASF mortars exhibit better resistance than OPC mortars against surface damage, although both systems get white deposits on the surface in phosphoric acid with a relatively high pH level. AASF mortars obtained lower mass loss than OPC mortars in phosphoric acid with pH at 2 and 3. The strength reduction in AASF mortars after immersion in phosphoric acid is more significant than that in OPC mortars. However, total degradation depth of AASF was smaller than that of OPC regardless of the pH of the acid solutions. Based on the experimental data, linear relationships were identified between the slope of degradation depth–mass loss curves and the Al/Si and Ca/Si ratios of the binders. This may indicate a new way to assess the degradation behavior of AASF and OPC based on their chemical compositions.

Keywords: alkali-activated materials, Portland cement, phosphoric acid, degradation, strength

OPEN ACCESS

Edited by:
Xiangming Zhou,
Brunel University London,
United Kingdom

Reviewed by:
Pengkun Hou,
University of Jinan, China
Bing Chen,
Shanghai Jiao Tong University, China

***Correspondence:**
Yingcan Zhu
yingcan.zhu@usq.edu.au
Zhenming Li
z.li-2@tudelft.nl

Specialty section:
This article was submitted to Structural Materials, a section of the journal Frontiers in Materials

Received: *29 December 2021*
Accepted: *21 February 2022*
Published: *09 March 2022*

Citation:
Ren J, Zhang L, Zhu Y, Li Z and San Nicolas R (2022) A Comparative Study on the Degradation of Alkali-Activated Slag/Fly Ash and Cement-Based Mortars in Phosphoric Acid. Front. Mater. 9:845349. doi: 10.3389/fmats.2022.845349

INTRODUCTION

Sewage wastewater environments containing various acids pose a significant threat to traditional ordinary Portland cement (OPC) concrete sewer pipes (De Belie et al., 2000; Bertron et al., 2004; Parande et al., 2006; Xiao et al., 2022a; Xiao et al., 2022b). Due to the alkaline nature of OPC binders, acid intrusion results in rapid neutralization reaction, leading to the dissolution and decomposition of some main components such as Portlandite, C-S-H gel, and ettringite (Oueslati and Duchesne, 2014). This causes an increase in porosity, decrease of mechanical strength of concrete, and corrosion of rebars embedded in concrete (Bertron et al., 2007; Aiken et al., 2018).

Related financial cost is associated with not only the maintenance and repair of damaged concrete structures but also the relative inaccessibility of sewage systems underground (Scrivener and De Belie, 2013) apart from some intangible costs because of road closure. In Hamburg (Germany), as early as 1970s, it was reported that 25 million euros were spent on the maintenance of sewer pipelines (Sydney et al., 1996). Today, in Australia, the annual cost of corrosion for pipelines is estimated to be $982 million, and the intangible costs could be up to 91 million annually for the urban water industry (Suzzanna, 2017). In China, due to the rapid industrialization and urbanization, the structural integrity and security of the large number of OPC concrete sewer pipes produced every year is raising concerns (Yang et al., 2014). Another issue related to the damage of sewage systems is the possible

leaching of various heavy and/or toxic metals either from the wastewater in the sewage pipes into surrounding soils or the other way around (Korboulewsky et al., 2002; Quenea et al., 2009). Moreover, the leaching of organotin compounds in the municipal sewer system can result in severe ecotoxicological consequences, and these compounds may even be responsible for bioaccumulation in the terrestrial food web, bringing potential damages to humans and other creatures (Fent, 1996). Therefore, it is important to find alternative materials with higher durability to be used in sewage pipes in order to reduce the cost caused by the degradation and related environmental impact.

Alkali-activated materials (AAMs) are a broad class of binding materials with alumina-silicate polymeric crosslinking structures (Mehta and Siddique, 2017; Longhi et al., 2020). They are manufactured by reactions between alumina/silica-containing solid sources and alkaline activators (such as sodium and potassium hydroxides and silicates) (Provis et al., 2015). The solid sources are usually industrial by-products, such as slag and fly ash (FA), making AAMs environmentally friendly as compared to OPC-based binders (Al Bakri Abdullah et al., 2012; Aiken et al., 2017; Messina et al., 2018; Ma et al., 2019). For instance, the production of one ton of OPC usually results in about 900 kg of CO_2 emissions (Pacheco-Torgal et al., 2012; Sata et al., 2012; Sánchez-Herrero et al., 2017; Coelho Martuscelli et al., 2018), while in comparison, AAMs are estimated to reduce CO_2 emissions by up to 80% (Deb et al., 2014). In addition, AAMs are endowed with excellent mechanical performance, high temperature resistance, and better resistance against chemical attacks such as sulfate compared to their OPC counterparts (Bakharev, 2005; Temuujin et al., 2011; Yan et al., 2017; Xie et al., 2019). In particular, it is believed that AAMs show superior durability to OPC-based binders in acid attacks because of the formation of decalcified but modified aluminosilicate gel which has been confirmed to delay the degradation process when exposed to acid attacks (Bernal et al., 2012; Ariffin et al., 2013; Ren et al., 2020a; Ren et al., 2022).

A few studies have been carried out to investigate the performance of AAMs exposed to sewer acidic environments (pH ranging between 2 and 6.5), particularly to sulfuric acid as it is the main cause of concrete corrosion in sewage environments (De Belie et al., 2004; Chang et al., 2005; Song et al., 2005; Albitar et al., 2017; Aiken et al., 2018; Ren et al., 2020b). However, apart from sulfate, many other anions are found in sewage effluent such as phosphate, nitrate, and chloride; for example, the phosphate concentration was above 5,000 ppm, which was much higher than that of sulfate (1,293 ppm), in some type of silage effluent (Aiken et al., 2017). Phosphates may be produced from phosphate-based fertilizers and artificial products such as synthetic detergents due to industrial and agricultural activities (Fuhs and Chen, 1975; Nagadomi et al., 2000). Therefore, it is also critical to explore the durability of concrete in phosphoric acid environments (acidic solution plus phosphates). Thus far, studies on this topic are very limited (Hanayneh et al., 2012; Ren et al., 2020a; Ren et al., 2020b; Ren et al., 2022). According to these preliminary studies (Ren et al., 2020b; Ren et al., 2022), alkali-activated slag/fly ash (AASF) pastes show higher resistance toward phosphoric acid than normal OPC counterparts. However, related works exploring the effect of different pH values of phosphoric acid on AAM mortars as alternatives to OPC systems are lacking.

Considering the earlier information, two types of AASF mortars were prepared in this study and immersed in phosphoric acid solutions with three pH levels for 150 days. An OPC-based mortar was used as reference. Specimens were visually inspected, and their mass changes were measured throughout the immersion period. The pore-related properties and compressive strength before and after acid immersion were investigated. Degradation depth over time was also measured. In addition, energy dispersive spectroscopy (EDS) analysis was conducted to identify the relationship between chemical composition and degradation behavior of the binders.

MATERIALS AND METHODS

Materials and Mixtures

Class F FA, according to ASTM C618, supplied by Cement Australia, and a ground granulated blast furnace slag (hereinafter termed slag) from Independent Cement and Lime Pty Ltd., Australia, were used as solid precursors for AASF. The slag had a specific gravity of 2.8 with a d_{50} of 14 μm, compared to 2.2 and 25 μm for the FA, respectively. AS 3972 type OPC (Eureka Cement, Australia), with a specific gravity of 2.8–3.2 and a bulk density of 1,400 kg/m^3, was used for manufacturing OPC-based samples. Chemical compositions of the raw materials used in the experiments are listed in **Table 1**. The fine aggregate used in the mortar preparation was premium-graded siliceous sand provided by SIBELCO, Australia, with a specific gravity of 2.55 and water absorption of 0.90%. The water absorption was determined in accordance with BS 812–2:1995. In this study, the siliceous sand used is not susceptible to acidic conditions (Zivica and Bajza, 2002).

Two AASF binders were prepared with the slag/FA ratios of 60/40 and 50/50 by mass, respectively, as these two ratios exhibited higher resistance against acid attacks than other ratios (Ren et al., 2020a; Ren et al., 2020b). The alkaline activator used was sodium metasilicate with a SiO_2/Na_2O molar ratio of 1.0 as supplied by redox. Two OPC-based binders were made, including one pure cement mortar (denoted as "100OPC") and blended OPC with 65% slag and 35% OPC (denoted as "65Slag_35OPC"), the latter of which was from our previous research (Ren et al., 2020b; Ren et al., 2022). AASF mixtures were formulated using different water-to-binder (w/b) ratios and different contents of solid alkaline activator to reach a similar target compressive strength (around 60 ± 5 MPa) after 56 days of curing. The purpose of fixing an identical targeted compressive strength and the same sand/binder ratio for all mortar mixes was to obtain a reasonable comparison regarding the durability of the four binder mixes (van Deventer et al., 2015). Specific mix proportions are shown in **Table 2**.

The alkaline activator solution for AASF mortar specimens was prepared by mixing the anhydrous sodium metasilicate particles with tap water. It was allowed to cool down naturally to room temperature (23 ± 2°C). Before adding the alkaline activator solution, the sand and other powder components of

TABLE 1 | Chemical compositions of slag, FA, and OPC determined by X-ray fluorescence. LOI is the loss on ignition at 1,000°C.

Precursor	Component (mass% as oxide)										
	SiO_2	TiO_2	Al_2O_3	Fe_2O_3	MnO	MgO	CaO	K_2O	P_2O_5	SO_3	LOI
Slag	31.00	0.49	13.96	0.32	0.33	6.33	40.92	0.31	0.01	2.17	2.11
FA	42.09	1.44	25.13	13.16	0.18	1.27	13.56	0.41	1.10	0.41	0.81
OPC	20.34	-	4.47	4.58	-	1.24	62.91	0.29	-	2.58	3.27

TABLE 2 | Mix proportions of AASF and OPC mortars.

Sample ID	Slag/FA ratio (%)[a]	Solid alkali/binder ratio (%)[a]	Water/binder ratio[a]	Sand/binder ratio[a]
60slag_40FA	60:40	7.5	0.38	2:1
50slag_50FA	50:50	8.0	0.36	
65slag_35OPC	—	—	0.44	
100OPC	—	—	0.42	

[a]*All values are given as mass ratios, "binder" refers to the cementitious materials including OPC, or slag and FA.*

each mixture including slag and FA or OPC were first dry mixed in a Hobart mixer (10 L capacity) for 2 min. Then the alkaline activator solution (for AASF) or water (for cement) was added into the dry mixture, with the mixing continued for 8 min. Newly mixed mortars were cast into two layers in different plastic cubic or cylindrical molds and compacted with a tamping rod on a vibrating table. The specimens were covered by plastic films for 24 h to minimize water loss and then demolded. AASF mortar specimens were sealed in plastic bags for 56 days, and OPC-based specimens were cured in water for the same duration prior to further experiments. All specimens were cured at room temperature (23 ± 2°C), and 56 days of curing was selected to minimize the influence of further hydration on the degradation measurements for all binder mixes (Ren et al., 2020b; Ren et al., 2020c; Ren et al., 2021).

Immersion in Phosphoric Acid

After 56 days of curing, mortar specimens were placed under ambient condition for 2 days to guarantee a similar saturation status. Then the samples were submerged in phosphoric acid solutions of three pH levels (2.0, 3.0, and 4.0) for 150 days. The pH selected was to mimic the severe aggressive environments of the sewage wastewater pipes (Larreur-Cayol et al., 2011; Ren et al., 2020b). Phosphoric acid solutions were renewed every day within 30 days of immersion and then renewed every 3 days between 30 and 56 days, after that the renewal frequency was every 5 days (before 90 days) and 7 days (after 90 days) until the end of immersion. The lower frequency used for acid replacement as time proceeded was due to a decreasing rate in pH increment after each replacement as measured by a digital pH meter (PHM210 Radiometer, Australia). One main reason for the pH fluctuation before each renewal of the solution was the consumption of hydronium by hydroxyls released from the binders (note that both AASF and OPC binders are alkaline) (Aiken et al., 2018). For each mortar mix in each solution, six replicated cylindrical samples (Φ 27.5 mm × H 55 mm) were immersed in a plastic container with 1 L of phosphoric acid. The solid/liquid volume ratio was kept at 0.20, and the solid surface area/liquid volume was 0.28 cm^{-1}. The top and bottom surfaces of the samples were sealed using silicone gel to ensure one-direction ingress of acid. Another three cubic samples (50 mm × 50 mm × 50 mm) were stored under the same condition with the purpose to measure the compressive strength (**Figure 1**).

For each mix, reference samples were prepared and submerged in water with the same exposure time. Water was also renewed every 3 days within the first month followed by a reduced frequency, with the pH ranging between 7.0 and 8.0.

Performance Characterization

Visual Inspection

The surfaces of samples immersed in phosphoric acid were photographed for visual inspection after 150 days of immersion. Samples were first taken out from acid, and the excessive solution on the surface was slightly wiped out, then the samples were dried at room temperature for 1 hour prior to visual inspections.

Mass Change

The mass of cylindrical samples was measured after 3, 7, 14, 21, 28, 35, 44, 60, 75, 90, 120, and 150 days of submersion in phosphoric acid solution or water. Three samples were used for each mortar mix at each age, and the averages were obtained. Before each measurement, samples were taken out from the phosphoric acid solution or water and wiped gently with a wet cloth. Each measurement was completed within 30 s followed by replacing the samples into the containers in the same orientation.

Capillary Sorptivity and Pore-related Properties

The capillary sorptivity test was conducted prior to the acid or water immersion. The rate of water ingress was measured by monitoring the mass gains of pre-dried samples over time with

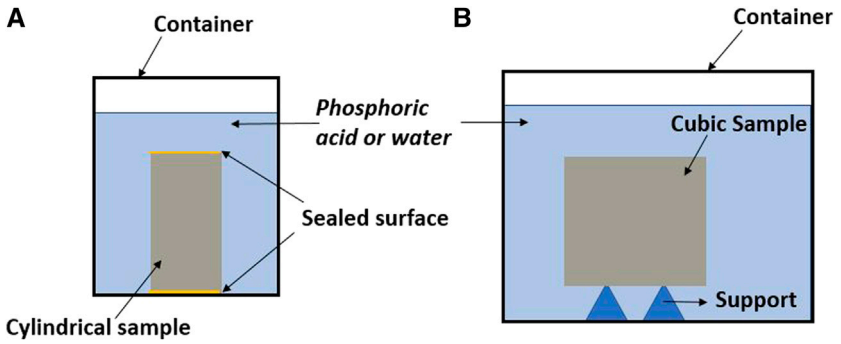

FIGURE 1 | Experimental setups for the immersion test, **(A)** cylindrical specimens (Φ 27.5 mm × H 55 mm) used for the measurements of mass, porous properties and degradation depth; **(B)** cubic specimens (50 mm × 50 mm × 50 mm) used for visual inspections and compressive strength test.

one surface contacting with water (ASTMC1585-04, 2004). The results can reflect the tendency of specimens to absorb and transmit water or acid solution *via* capillarity actions. It is worth noting that capillary sorptivity is not only dependent on porosity but also associated with pore size distributions and connectivity of pores (Pavía and Condren, 2008; Lee and Lee, 2016). The capillary sorptivity test was performed based on ASTM C1585-04 (ASTMC1585-04, 20) using three disk-shaped specimens (50 mm diameter and 10 mm height) for each mortar mixture. Detailed testing procedures can be referred to other studies (Albitar et al., 2017; Ren et al., 2019).

The permeable porosity of the mixtures before and after immersion was measured in compliance with ASTM C642-06 (CASTM 642 (2006), Standa, 2006). Three cylindrical samples (Φ 27.5 mm × H 55 mm) were used for each mix and each exposure condition. The samples were first oven-dried at 60°C until a constant mass was achieved. Drying at 110°C was not adopted due to the possible damages on the pore structures of AASF binders (Ismail et al., 2013). It is worth pointing out that due to the severe damages on the samples in phosphoric acid with pH at 2, the permeable porosity test was not performed on those samples. The volume of permeable voids (VPV) can be quantified based on the calculation methods described in previous studies (Ren et al., 2019; Guo et al., 2021) based on different mass values of specimens measured under various conditions.

Compressive Strength

The compressive strength of all mortar mixes after 56 days of curing prior to submersion in phosphoric acid solutions or water was determined on cubic samples according to ASTM C109M (AASTM, 1999). After 150 days of immersion in different pH environments, the compressive strength of all mortar mixes was measured again. Triplicates of each mix after exposure were tested to obtain average readings.

Degradation Depth

The degradation depth of the mixes due to acid ingress was measured after 3, 7, 11, 14, 21, 28, 35, 44, 60, 75, 90, 120, and 150 days of immersion. Immersion in water did not cause any apparent degradation of the sample; therefore, total degradation depth of the mixtures in water was not measured. Six cylindrical samples of each mortar mix were used for each pH condition throughout the immersion period. A slice of about 5 mm was cut off from each cylindrical sample using a diamond saw. After that, the surface of the slice was cleaned with distilled water and dried naturally in the ambient environment; then a phenolphthalein solution was sprayed onto the plane surface and the color change was the criterion used to distinguish the degraded region surrounding the undegraded core (delineated by reaction front in **Figure 2**). The pink/violet color indicates a pH higher than 8.3, with dark and light violet corresponding to pH > 10.0 and 8.3 < pH < 10, respectively. The uncolored area is considered as the degraded part, with the thickness expressed as neutralized depth (*ND*). Sample surfaces were first observed using an optical video microscope, and the images were processed with the MATLAB image processing toolbox so that *ND* can be determined with

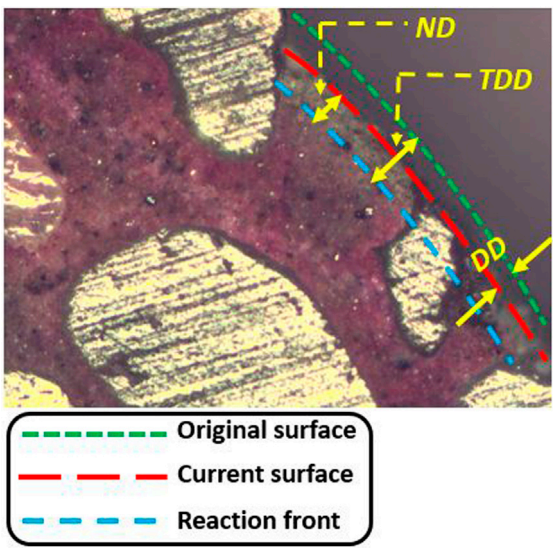

FIGURE 2 | Illustration of ND, DD, and TDD in a microscope image of 50Slag_50FA sample surface after the spray of phenolphthalein (immersion age was 28 days and the pH of acid was 4.0).

TABLE 3 | Porous properties and compressive strength of the four mortar mixes after 56 days of curing.

Sample ID	Porous properties			Compressive strength (MPa)
	Water absorption (%)	VPV (%)	Capillary sorptivity ($mm/min^{0.5}$)	
60slag_40FA	6.68 ± 0.27	14.64 ± 0.57	0.52 ± 0.03	57.69 ± 0.88
50slag_50FA	6.58 ± 0.17	14.26 ± 0.38	0.52 ± 0.05	56.65 ± 1.73
65slag_35OPC	10.11 ± 0.38	20.79 ± 0.66	0.09 ± 0.01	56.92 ± 1.54
100OPC	8.32 ± 1.52	15.15 ± 0.08	0.51 ± 0.02	60.50 ± 3.86

relatively high precision. For each sample slice, the *ND* value was obtained from five points randomly distributed around the circumference.

In addition, the dissolved and/or detached depth (*DD*) was also taken into account due to the partial dissolution of the degraded part, also performed by Larreur-Cayol et al. (2011). The *DD* value was obtained by measuring the initial diameter and the current diameters at different time intervals. Then the *DD* was deduced from the formula:

$$DD = \frac{D_0 - D_i}{2} \ (i = 1, 2, 3...), \tag{1}$$

where *DD* is the dissolved/detached depth, D_0 is the initial diameter of the sample which was 27.5 mm in this study. D_i is the diameter after each immersion period. For example, D_1 is the averaged diameter when the first diameter measurement was performed after 3 days of immersion. *DD* was measured before the corresponding *ND* measurements, expressed as the average of six samples for each mix at each pH condition.

The total degradation depth (*TDD*), denoted as "degradation depth," was the sum of two parts: $TDD = DD + ND$, as illustrated in **Figure 2**. According to different mechanisms, a greater *ND* reflects a higher alkalinity loss, whereas a greater *DD* indicates more structural mass loss caused by dissolution and/or decomposition of mortar samples due to acid immersion.

Energy Dispersive Spectroscopy Analysis

After 150 days immersion in phosphoric acid with pH at 2.0, sample surfaces were examined by using environmental scanning electron microscopy (ESEM), using an FEI Quanta instrument at a 15 kV accelerating voltage. Polished samples were evaluated in a low vacuum mode using a backscatter detector to avoid the need for carbon coating of the samples. A LINK-ISIS (Oxford Instruments) energy-dispersive X-ray (EDX) detector was used to determine the chemical compositions of both the degraded and undegraded part of the sample. From each region, 20 points were selected within the binder matrix excluding unreacted slag, FA, and OPC particles as well as sand.

RESULTS AND DISCUSSION

Characterization Prior to Acid Immersions

The compressive strength and pore-related properties including water absorption, VPV, and capillary sorptivity prior to the acid exposure are shown in **Table 3**. It is apparent that all mortar mixes obtained similar compressive strength (58 ± 2 MPa) after 56 days, based on which their durability can be reasonably compared. 65Slag_35OPC obtained the highest water absorption (10.11%) and VPV (20.79%), which is closely associated with the largest amount of water used for manufacturing followed by those of 100OPC specimens. The two AASF mortar samples displayed lower water absorption and VPV values because of less water usage than OPC-based counterparts (**Table 3**), indicating less volume of voids than that of the OPC-based specimens.

In terms of capillary sorptivity, 65Slag_35OPC exhibited much lower capillary sorptivity than AASF mortars and 100OPC despite its highest water absorption and VPV, which was only 0.09 $mm/min^{0.5}$. This can be explained by considering their different pore size distributions: it is possible that 65Slag_35OPC contained much fewer large capillary pores (sizes greater than 200 nm) than the other binders. According to Lee and Lee (2016), there are three stages of water absorption and capillary sorptivity calculated from the slope of the first stage where it is the macropores larger than 200 nm in diameter that control the water absorption rate. Therefore, the capillary sorptivity of 65Slag_35OPC was much lower than that of the other binders. At the same time, it may have a higher volume of mesopores or gel pores with pore sizes less than 200 nm in diameter, contributing to its largest water absorption and VPV. Another possible reason can be the slow but continuous hydration of 65Slag_35OPC because of the addition of slag so that the connectivity of pores substantially decreased. This led to a much lower capillary sorptivity than 100OPC since sorptivity is also relevant to the connectivity of porous structures (Tang et al., 2016; He et al., 2018).

Performance Degradation After Acid Immersions

Visual Appearances

The appearances of samples after 150 days of immersion in the phosphoric acid and water are shown in **Figure 3**. After immersion in water, as shown in **Figure 3A**, all binders remained intact with a smooth surface and original sharp edges.

When the pH of the acid is 2.0, as presented in **Figure 3B**, AASF mortar samples seemed to have no obvious signs of degradation, such as discolorations, compared to the control samples submerged in water. In contrast, it is apparent that the OPC-based mortar mixes were severely degraded

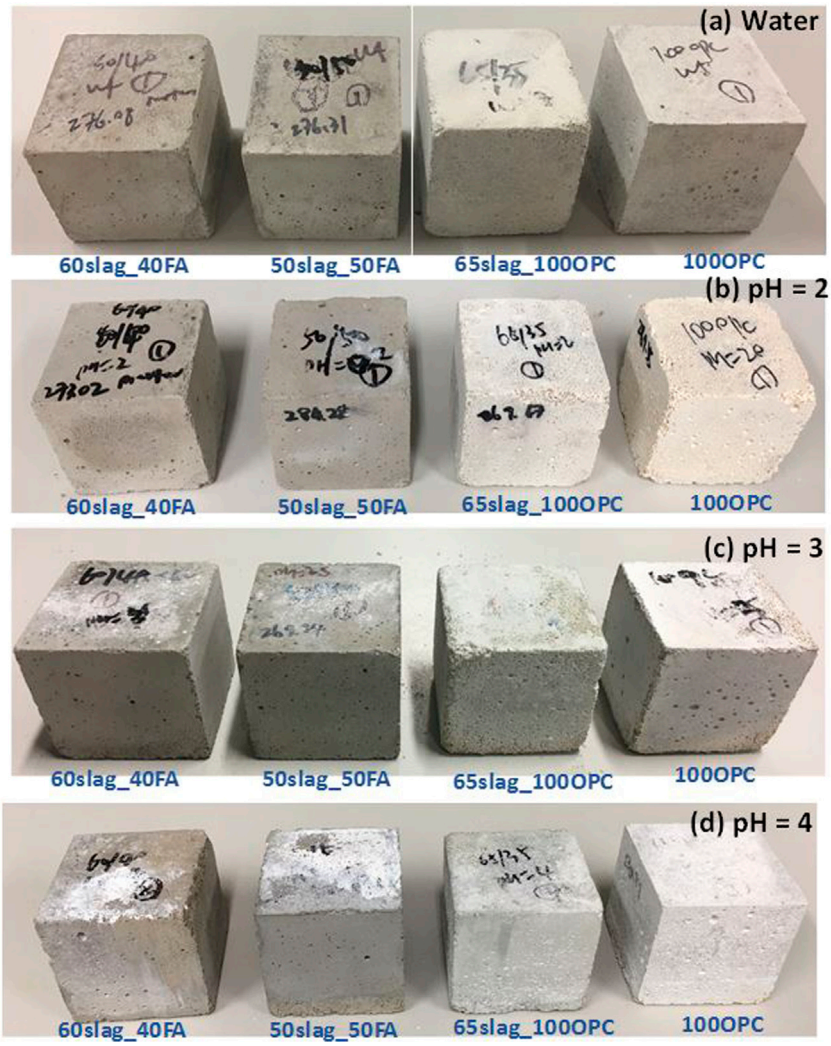

FIGURE 3 | Appearances of mortar mixes after immersion in phosphoric acid for 150 days with different pH levels: **(A)** pH = 2.0, **(B)** pH = 3.0, **(C)** pH = 4.0 and **(D)** in water with pH = 7.0.

evidenced by their rough and soft surfaces (particularly around the edges of the samples), due to mortar spalling and less mechanical sound binder. In particular, some shallow holes were visible on the surface of the 100OPC sample. The surface appeared to be more yellowish/brown than the sample after immersion in water, consistent with the findings in other studies (Bertron et al., 2004; Aiken et al., 2017; Muthu and Santhanam, 2018). This color can be attributed to a higher relative content of ferrite in the surface layer or the formation of new iron-containing precipitation since Fe is a favorable element for resistance toward acid attacks (Bertron et al., 2005a; Muthu and Santhanam, 2018). Furthermore, OPC-based samples were found softer in touch than AASF binders, indicating lower resistance of OPC against strong acid.

When the acid pH was 3.0 (**Figure 3C**), white compounds on the surfaces of all binder mixes were observed, which was likely due to the formation of calcium phosphates, such as brushite ($CaHPO_4{\cdot}2H_2O$) (Aiken et al., 2017). In addition, some "pin-hole"-like voids on the surface of 100OPC appeared due to binder dissolution after exposing to the acid. Furthermore, an increased roughness of edges of 65Slag_35OPC was also observable. In comparison, AASF mortar samples did not present obvious damage.

When the pH of the acid was four (**Figure 3D**), more white compounds were noticed on the surfaces of samples than when the scenario of pH at 3, especially for AASF and 100OPC samples. No apparent damage was observed on AASF samples. The edges of the OPC-based samples were more intact than the ones in acid with higher aggressivity.

The results in **Figure 3** show two types of visible performance changes due to exposure to the phosphoric acid solutions, which is the precipitation of white reaction products and rough surfaces and edges. These two effects seemed to occur concurrently. For AASF binders, no obvious signs of damage were observed, and

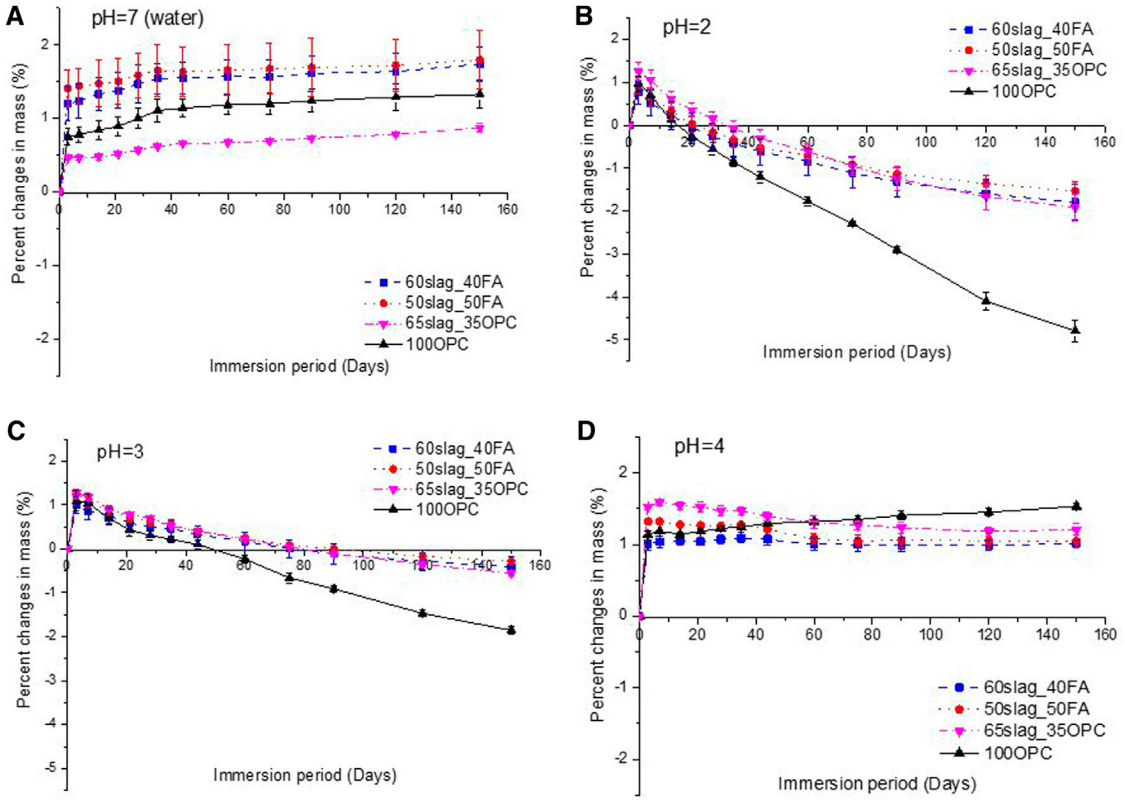

FIGURE 4 | Mass changes of mortars over 150-day immersion in water (pH = 7) **(A)** and in phosphoric acid with pH = 2 **(B)**, pH = 3 **(C)** and pH = 4 **(D)**. Positive and negative values indicate mass gain and loss, respectively.

the precipitation effect was more noticeable when the pH value increased. For OPC-based binders, the degradation was more prominent, but the precipitation was less distinguishable when exposed to the acid with lower pH values. One probable reason for this phenomenon is that the calcium phosphates at pH 2 tend to dissolve in the acid solution rather than to deposit on the sample surfaces. By visual observations, it is evident that AASF-based samples present fewer deteriorations in phosphoric acid than the OPC-based binders as consistent in other studies, in which different acids were involved (Aiken et al., 2017; Albitar et al., 2017; Aiken et al., 2018).

Mass Changes

Figures 4A–D show the mass changes of the mortar mixes over time in the phosphoric acid solutions and water. Within the first 3 days, all samples obtained mass gains because of water ingress. Although the samples were cured under sealed condition rather than drying condition before immersion, self-desiccation would induce a decreasing saturation degree of the sample with time; thus, water absorption occurs when exposed to solutions.

After the first 3 days, the mass of mortars in water continuously increased before reaching a plateau after about 44 days (**Figure 4A**). By contrast, the mass of all mixtures in the acid of pH at 2 and 3 started to decrease after 3 days (**Figures 4B,C**). In general, the mass loss of all samples was higher in pH at 2. In both solutions, 100OPC showed the most rapid mass loss, which was nearly linear with time. A similar trend was observed for OPC concrete exposed to sulfuric acid (Albitar et al., 2017). After 150 days, the mass loss of 100OOPC reached around 5 and 2% in pH at 2 and 3, respectively. The significant mass loss of 100OPC is consistent with its visual damage as shown in **Figures 3B,C**. In contrast, the mass loss for the other three types of binders decelerated gradually with time. The lower mass loss of AASF binders can be attributed to the formation of an insoluble or a less soluble degraded layer acting as a barrier toward the ingress of acid solutions as reported by Bernal et al. (2012). For 65slag_35OPC, it is possible that some reaction products such as brushite (Ren et al., 2022) blocked the tortuous capillary pores, and thus, the mass loss caused by the phosphoric acid attack became less gradual. The results in **Figure 4** suggest that AASF binders displayed higher phosphoric acid resistance than OPC-based binders when pH was at 2–3.

When pH was at four (**Figure 4D**), the mass loss of AASF after the first 3 days was not significant. 100OPC even experienced a slight increase in mass, which can be attributed to the continuous hydration of cement given a limited damage of the sample by acid (**Figure 3C**). The formation of white compounds on the surface may also contribute to the mass gain.

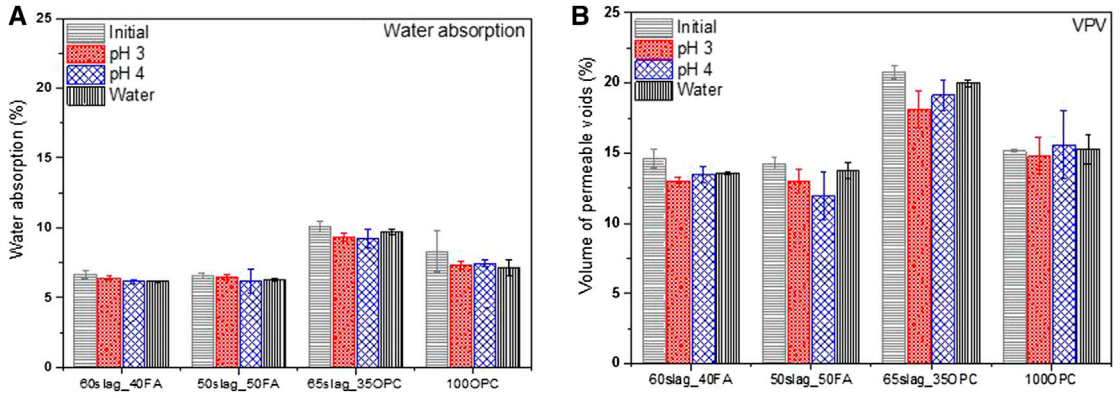

FIGURE 5 | Water absorption and VPV before and after 150-day immersion in the phosphoric acid solutions (pH = 3 and 4) and in water (pH = 7).

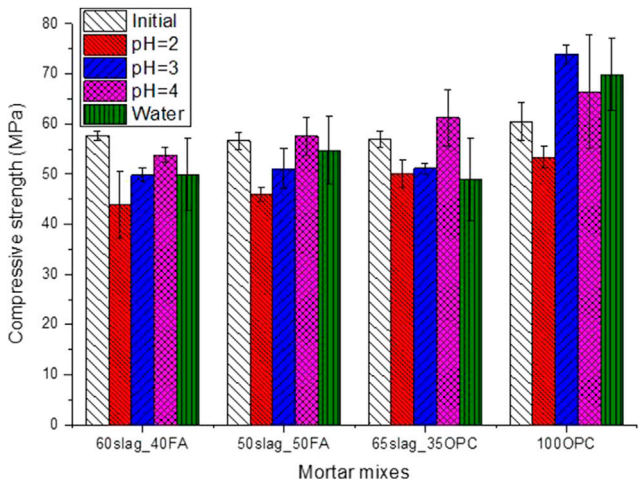

FIGURE 6 | Compressive strength of the four mortar mixes after 150-day exposure in phosphoric acid solutions with different pH values and in water as reference.

Pore-Related Properties

Figure 5 shows the water absorption and VPV of the mixtures before and after 150 days of immersion. The water absorption of AASF binders did not change significantly despite the type of solutions. Although some white deposits formed on the surface of AASF immersed in acid of pH at three and four (**Figure 3**), their influences on the water absorption seem minor. 100OPC mixture showed lower water absorption after immersed in water due to the continuous hydration, and thus, the pore structure was more densified. Acid ingress damaged the structure of OPC; hence, the decrease in water absorption during immersion was counterbalanced.

As shown in **Figure 5B**, the two AASF binders displayed a decrease in VPV irrespective of the pH values, indicating the possible deposition of reaction products such as calcium phosphates. This corresponds well with the white compounds observed on the surface of the AASF samples after immersion (**Figure 3**). It is possible that the white compound was a chemical reaction product involved in the precipitation on the surface pores, thus leading to reduced VPV values. Similar phenomenon was reported in another study on the sulfuric acid attacks, which confirmed that the reaction mainly occurs on the sample surface with products blocking pores (Kawai et al., 2005). The inconsistent results between water absorption and VPV indicate that VPV is more sensitive to the precipitation effect. In comparison, 100OPC experienced a smaller decrease or even increment after submersion in acid, indicating a hindered densification or coarsened porosity due to acid attack. It is reasonable since OPC contains more reactive calcium than AASF binders so that more products were dissolved at a high concentration of hydroniums.

Compressive Strength

The compressive strengths of different mortar mixes after 150 days of immersion in different conditions are shown in **Figure 6**. For AASF-based binders, acid of pH at 2 and 3 caused reduction in the compressive strength, while pH at 4 seemed to be not so aggressive. These results are in line with the

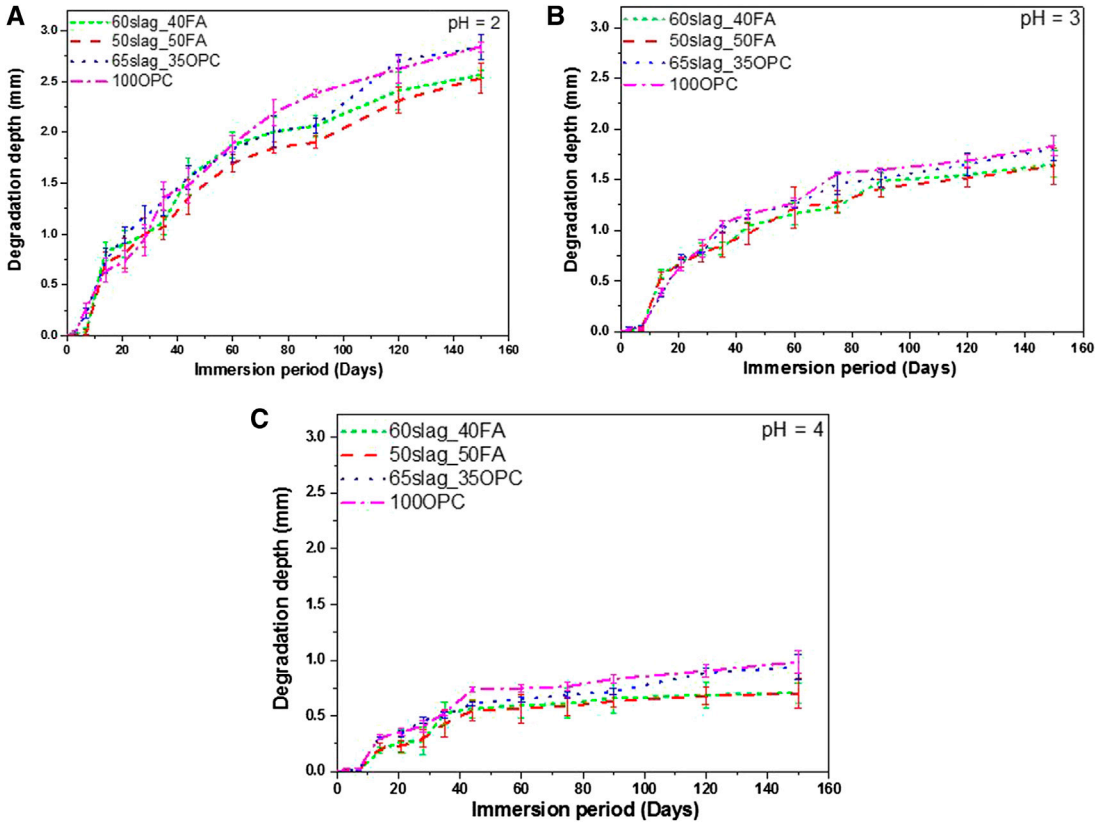

FIGURE 7 | Total degradation depth evolution over 150-day immersion period for the four mortar mixes exposed phosphoric acid with **(A)** pH = 2; **(B)** pH = 3; and **(C)** pH = 4.

mass changes, which show that little change in mass can be observed for pH at 4, whereas pH at 2 and 3 resulted in obvious mass losses after 150 days of exposure. Immersing in water, interestingly, also caused strength reduction of AASF. This is probably due to the leaching of ions from the pore solution or even solid products. The reduction of around 10% in strength due to immersion in water is similar to what had been reported in another literature (Huang et al., 2018). The reason why pH at 4 was even better than water in terms of strength has not been clearly understood, which is probably associated with the reaction products after degradation clogging the pores and thus impeding the ion leaching process.

For 100OPC, strength increase was observed except for pH at 2. The increase of the compressive strength in water is probably due to further hydration during 150 days of immersion. The higher strength of 100OPC in pH at 3 than at 4 is consistent with the lower VPV of the mixture in pH at 3, as shown in **Figure 5**, which might be due to the formation of more phosphates precipitated in the specimens such as brushite (Ren et al., 2022). The acid with pH at 2 seemed too aggressive to maintain the structural integrity of OPC. The large standard deviation when pH was at 4 was possibly related to the unevenly distributed degradation reaction products on specimens.

Figure 6 shows that OPC had higher strength than AASF in all conditions, although the acid induced more visual damage (**Figure 3**) and higher mass loss (**Figure 4**) for OPC. These seeming contradictory results are due to the fact that visual damage and mass loss occurred mainly on the surface of the samples, while the strength was dependent also on the core part which was relatively intact. This point will be further verified in the next section.

Degradation Depth

Figure 7 shows total degradation depth (TDD) evolution within 150 days of immersion in phosphoric acid. In general, the stronger the acid (lower pH values) was, the larger degradation depth was observed for all mixtures. The results are in accordance with the findings from other studies that lower pH values of acids would usually result in greater degradation depths (Bertron et al., 2005b; Lloyd et al., 2012). Within the first 7 days of immersion, very small degradation depth was seen, whereas a significant increase was observed soon after, followed by a gradually decreasing rate in the development of degradation depth until the end of immersion. This phenomenon was also reported in a previous study on paste mixtures (Ren et al., 2020b). Within 150 days, total degradation depth of all mixes was within 3 mm, indicating that the degradation basically occurred in the surface, rather than the whole sample.

For all pH conditions (pH at 2, 3, and 4) at the end of exposure, the increasing order of total degradation depth is the same:

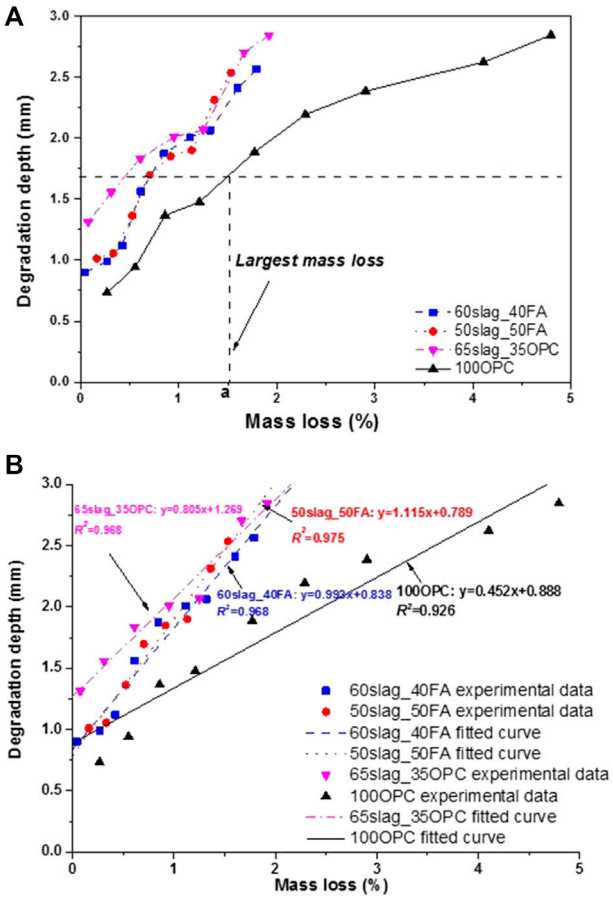

FIGURE 8 | (A) The relationship between total degradation depth (mm) and mass loss (%) for all mortar mixes during the exposure in the phosphoric acid with pH at 2. Note: the plot only includes mass losses (no mass gains) and their corresponding degradation depth. **(B)** Linear fitting of the curves.

50Slag_50FA ≈ 60Slag_40FA < 65Slag_35OPC <100OPC, corresponding well with the mass losses when pH was at 2 and 3 (**Figure 4**). The results indicate that AASF mortars exhibited better resistance than OPC mortars against the ingress of phosphoric acid, while **Figure 6** shows that the strength of OPC samples was actually higher. When it comes to the evaluation of durability of AASF and OPC, an overall consideration of different performances is needed. However, as to the role of concrete as the protection of steel rebar, it seems the AASF system is a better choice than the OPC with comparable 56-day strength.

Relationship Between Degradation Depth and Mass Loss

The mass losses and corresponding degradation depths for the four mortar mixes exposed to the phosphoric acid (pH = 2) are plotted in **Figure 8A**. It is apparent that total degradation depth becomes greater as the mass loss increases, regardless of mortar types. This is reasonable because mass losses due to dissolution and decomposition can be reflected by the dissolved depth (DD), as a part of degradation depth. Moreover, at the same degradation depth (e.g., shown as the horizontal dash line in **Figure 8A**), it is apparent that 100OPC sample suffers the greatest mass loss (marked "a" value on *x*-axis). Thus, it is possible to conclude that the 100OPC sample is more likely to experience great structural disintegrations, which can be attributed to successive decomposition and/or dissolution of main hydration products in OPC binders such as Portlandite, ettringite, and C-S-H gels (Oueslati and Duchesne, 2014). In comparison, 65Slag_35OPC and AASF-based binders tend to obtain much smaller mass losses. It is possible to associate this difference to the different relative aluminum contents in these systems. It is reported that gels with higher aluminum are more resistant to acid attacks because of the intensive cross-linked networks (Bernal et al., 2012; Varga et al., 2015). According to Bernal et al. (2012), the degraded layer of alkali-activated slag mortars, which is mainly composed of aluminosilicates, is still relatively compact after the acid attacks instead of the highly porous silica-rich gel for pure OPC mortars. Another study confirmed that AASF binders displayed less mass loss than OPC under silage effluent attack due to their higher Al/Si and lower Ca/Si ratios (Aiken et al., 2017).

TABLE 4 | Al/Si and Ca/Si atomic mass ratios of samples based on EDX analysis.

Sample ID	*Undegraded part*		*Degraded part*		"*k*"-slope
	Al/Si	Ca/Si	Al/Si	Ca/Si	
60slag_40FA	0.52 ± 0.03	1.00 ± 0.07	0.48 ± 0.03	0.09 ± 0.01	0.993
50slag_50FA	0.55 ± 0.02	0.87 ± 0.02	0.52 ± 0.04	0.08 ± 0.03	1.115
100OPC	0.24 ± 0.04	1.40 ± 0.33	0.30 ± 0.06	0.71 ± 0.02	0.452

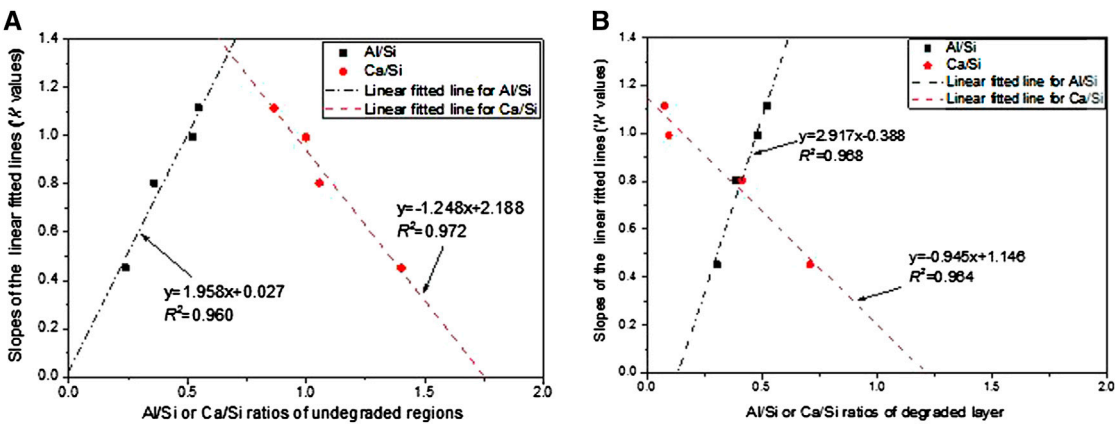

FIGURE 9 | Al/Si and Ca/Si ratios in the **(A)** undegraded layer and **(B)** degraded layer of the four different mortar mixes.

To confirm the relationship between chemical composition and degradation depth, the Al/Si and Ca/Si ratios in both the undegraded and degraded layers of the samples immersed for 150 days with pH at 2 were measured by EDX, and the results are listed in **Table 4**. Moreover, the slope *k* values of the linearly fitted degradation depth-mass loss curves (**Figure 8B**) are also listed in **Table 4** for the convenience of comparison. The Al/Si ratios for the two AASF-based binders are higher than those of the 100OPC binder. The opposite is true for the Ca/Si ratios. The Al/Si ratio shows a slight decrease for AASF mortar samples (i.e., from 0.52 to 0.48 for 60Slag_40FA) and an increase for OPC (from 0.24 to 0.30) when the area transforms from the undegraded to degraded part of the samples. By contrast, Ca/Si had a significant decrease for all mixes, indicating a much higher vulnerability of Ca than Al when exposed to phosphoric acid attacks. From **Table 4**, it can also be seen that the *k* values of the fitted lines correspond well with Al/Si and Ca/Si ratios: a higher Al/Si or a lower Ca/Si corresponds to a larger *k* regardless of the region (degraded or undegraded).

The correlation between *k* values and the Al/Si or Ca/Si ratios in the two areas is further fitted linearly, as shown in **Figure 9**. It is interesting to find that despite the changes in the chemical composition due to acid ingress, the Al/Si and Ca/Si ratios always have linear relationship with *k*. This suggests a way to roughly assess the relative degradation resistance of different binders against phosphoric acid, that is, total degradation depth against mass loss, by the chemical compositions of the binder. A higher Al/Si ratio and a lower Ca/Si ratio would lead to larger degradation depth under the same mass loss, or a lower mass loss when total degradation depth is the same. This point was also supported by the results in the study by Aiken et al. (2017). The comparison in **Figure 9** shows that the R^2 value for Ca/Si of the undegraded layer (R^2 = 0.972) is higher than that of the degraded layer (R^2 = 0.964), whereas the R^2 value for Al/Si shows an opposite result (0.960 and 0.968, respectively). This implies that Ca/Si in the undegraded layer and Al/Si in the degraded layer are more representative in reflecting the resistance to structural disintegrations.

The results in this study provide a possible method to predict the degradation kinetics when only mass loss or degradation depth could be obtained, especially after a long immersion period. In addition, this result shows that the resistance of binders against mass loss when suffering from acid attacks seems to be determined by Al/Si (degraded layer) and Ca/Si (undegraded layer) ratios irrespective of the binder types.

CONCLUSION

In this study, the degradation behavior of AASF and OPC mortars against phosphoric acid was investigated and compared. Based on the results, the following conclusions can be drawn:

- Two types of visible performance variations of AASF and OPC mortars exposed to phosphoric acid solutions were observed, which are the precipitation of white reaction products and rough surfaces and edges.
- While the OPC mortar showed surface damages, especially in strong phosphoric acid, no obvious signs of damages were

observed for AASF mortars. However, precipitation of white products was noticeable on both systems when the pH value increased.

- All mixes showed severer mass loss in phosphoric acid with decreased pH values. The OPC mortar showed higher mass loss than AASF mortars in phosphoric acid with pH at 2 and 3. In phosphoric acid with pH at 4, however, OPC showed mass gain due probably to the precipitation of deposits.
- The strength reduction in AASF mortars was more than that in the OPC mortar but less than that in the slag-OPC blended mortar. However, total degradation depth of AASF was less than that of OPC in all pH levels of acid solutions.
- Linear relationships were identified between the slope of degradation depth-mass loss curves and the Al/Si and Ca/Si ratios of the binder. The statistical data indicate a new, maybe rough, way to assess the degradation behavior of AASF and OPC based on their intrinsic chemical compositions.

DATA AVAILABILITY STATEMENT

The original contributions presented in the study are included in the article/Supplementary Material, further inquiries can be directed to the corresponding author.

AUTHOR CONTRIBUTIONS

JR: experimental investigation, writing—original draft, and funding acquisition; LZ: supervision, writing—review &amp, and editing; YZ: resources, writing—review &amp, and editing; ZL: methodology, formal analysis, writing—review &amp, and editing; RSN: conceptualization, methodology, project administration, funding acquisition, and supervision.

FUNDING

The first author of this study was supported by the Australian Research Council (ARC IH150100006) and the Chinese Scholarship Council (CSC).

ACKNOWLEDGMENTS

The experimental work was carried out in the Geopolymer and Minerals Processing Group laboratory of the department of Infrastructure Engineering at the University of Melbourne. The assistance of laboratory research assistant Laura Jukes is also acknowledged here.

REFERENCES

AASTM, C109/C109M-Standard Test Method for Compressive Strength of Hydraulic Cement Mortars (Using 2-in. Or (50-mm) Cube Specimens); 2013. 2 (1999).

Aiken, T. A., Kwasny, J., Sha, W., and Soutsos, M. N. (2018). Effect of Slag Content and Activator Dosage on the Resistance of Fly Ash Geopolymer Binders to Sulfuric Acid Attack. *Cement Concrete Res.* 111, 23–40. doi:10.1016/j.cemconres.2018.06.011

Aiken, T. A., Sha, W., Kwasny, J., and Soutsos, M. N. (2017). Resistance of Geopolymer and Portland Cement Based Systems to Silage Effluent Attack. *Cement Concrete Res.* 92, 56–65. doi:10.1016/j.cemconres.2016.11.015

Al Bakri Abdullah, M. M., Hussin, K., Bnhussain, M., Ismail, K. N., Yahya, Z., and Razak, R. A. (2012). Fly Ash-Based Geopolymer Lightweight concrete Using Foaming Agent. *Int. J. Mol. Sci.* 13, 7186–7198. doi:10.3390/ijms13067186

Albitar, M., Mohamed Ali, M. S., Visintin, P., and Drechsler, M. (2017). Durability Evaluation of Geopolymer and Conventional Concretes. *Construction Building Mater.* 136, 374–385. doi:10.1016/j.conbuildmat.2017.01.056

Ariffin, M. A. M., Bhutta, M. A. R., Hussin, M. W., Mohd Tahir, M., and Aziah, N. (2013). Sulfuric Acid Resistance of Blended Ash Geopolymer concrete. *Construction Building Mater.* 43, 80–86. doi:10.1016/j.conbuildmat.2013.01.018

AstmC1585-04(2004). *Standard Test Method for Measurement of Rate of Absorption of Water by Hydraulic-Cement Concretes*. ASTM International.

Bakharev, T. (2005). Durability of Geopolymer Materials in Sodium and Magnesium Sulfate Solutions. *Cement Concrete Res.* 35 (6), 1233–1246. doi:10.1016/j.cemconres.2004.09.002

Bernal, S. A., Rodríguez, E. D., Mejía de Gutiérrez, R., and Provis, J. L. (2012). Performance of Alkali-Activated Slag Mortars Exposed to Acids. *J. Sust. Cement-Based Mater.* 1 (3), 138–151. doi:10.1080/21650373.2012.747235

Bertron, A., Duchesne, J., and Escadeillas, G. (2005). Accelerated Tests of Hardened Cement Pastes Alteration by Organic Acids: Analysis of the pH Effect. *Cement Concrete Res.* 35 (1), 155–166. doi:10.1016/j.cemconres.2004.09.009

Bertron, A., Duchesne, J., and Escadeillas, G. (2005). Attack of Cement Pastes Exposed to Organic Acids in Manure. *Cement and Concrete Composites* 27 (9-10), 898–909. doi:10.1016/j.cemconcomp.2005.06.003

Bertron, A., Duchesne, J., and Escadeillas, G. (2007). Degradation of Cement Pastes by Organic Acids. *Mater. Struct.* 40 (3), 341–354. doi:10.1617/s11527-006-9110-3

Bertron, A., Escadeillas, G., and Duchesne, J. (2004). Cement Pastes Alteration by Liquid Manure Organic Acids: Chemical and Mineralogical Characterization. *Cement Concrete Res.* 34 (10), 1823–1835. doi:10.1016/j.cemconres.2004.01.002

CASTM, 642 (2006). *Standard Test Method for Density, Absorption, and Voids in Hardened concrete*, 4. Annual book of ASTM standards.

Chang, Z.-T., Song, X.-J., Munn, R., and Marosszeky, M. (2005). Using limestone Aggregates and Different Cements for Enhancing Resistance of concrete to Sulphuric Acid Attack. *Cement Concrete Res.* 35 (8), 1486–1494. doi:10.1016/j.cemconres.2005.03.006

Coelho Martuscelli, C., Cesar dos Santos, J., Resende Oliveira, P., Hallak Panzera, T., Paulino Aguilar, M. T., and Thomas Garcia, C. (2018). Polymer-cementitious Composites Containing Recycled Rubber Particles. *Construction Building Mater.* 170, 446–454. doi:10.1016/j.conbuildmat.2018.03.017

De Belie, N., Lenehan, J. J., Braam, C. R., Svennerstedt, B., Richardson, M., and Sonck, B. (2000). Durability of Building Materials and Components in the Agricultural Environment, Part III: Concrete Structures. *J. Agric. Eng. Res.* 76 (1), 3–16. doi:10.1006/jaer.1999.0520

De Belie, N., Monteny, J., Beeldens, A., Vincke, E., Van Gemert, D., and Verstraete, W. (2004). Experimental Research and Prediction of the Effect of Chemical and Biogenic Sulfuric Acid on Different Types of Commercially Produced concrete Sewer Pipes. *Cement Concrete Res.* 34 (12), 2223–2236. doi:10.1016/j.cemconres.2004.02.015

Deb, P. S., Nath, P., and Sarker, P. K. (2014). The Effects of Ground Granulated Blast-Furnace Slag Blending with Fly Ash and Activator Content on the Workability and Strength Properties of Geopolymer concrete Cured at Ambient Temperature. *Mater. Des.* (1980-2015) 62 (62), 32–39. doi:10.1016/j.matdes.2014.05.001

Fent (1996). Organotin Compounds in Municipal Wastewater and Sewage Sludge : Contamination, Fate in Treatment Process and Ecotoxicological Consequences. *Sci. Total Environ.* 185 (1-3), 151–159. doi:10.1016/0048-9697(95)05048-5

Fuhs, G. W., and Chen, M. (1975). Microbiological Basis of Phosphate Removal in the Activated Sludge Process for the Treatment of Wastewater. *Microb. Ecol.* 2 (2), 119–138. doi:10.1007/bf02010434

Guo, S.-Y., Luo, H.-H., Tan, Z., Chen, J.-Z., Zhang, L., and Ren, J. (2021). Impermeability and Interfacial Bonding Strength of TiO2-Graphene Modified Epoxy Resin Coated OPC concrete. *Prog. Org. Coat.* 151, 106029. doi:10.1016/j.porgcoat.2020.106029

Hanayneh, B., Shatarat, N., and Katkhuda, H. (2012). Improving Durability of concrete to Phosphoric Acid Attack. *Jordan J. Civil Eng.* 6, 68–82.

He, R., Ma, H., Hafiz, R. B., Fu, C., Jin, X., and He, J. (2018). Determining Porosity and Pore Network Connectivity of Cement-Based Materials by a Modified Non-contact Electrical Resistivity Measurement: Experiment and Theory. *Mater. Des.* 156, 82–92. doi:10.1016/j.matdes.2018.06.045

Huang, G., Ji, Y., Zhang, L., Li, J., and Hou, Z. (2018). The Influence of Curing Methods on the Strength of MSWI Bottom Ash-Based Alkali-Activated Mortars: The Role of Leaching of OH− and Free Alkali. *Construction Building Mater.* 186, 978–985. doi:10.1016/j.conbuildmat.2018.07.224

Ismail, I., Bernal, S. A., Provis, J. L., Hamdan, S., and van Deventer, J. S. J. (2013). Drying-induced Changes in the Structure of Alkali-Activated Pastes. *J. Mater. Sci.* 48 (9), 3566–3577. doi:10.1007/s10853-013-7152-9

Kawai, K., Yamaji, S., and Shinmi, T. (2005). "Concrete Deterioration Caused by Sulfuric Acid Attack," in International Conference on Durability of Building Materials and Components (Lyon: LYON [France]), 17–20.

Korboulewsky, N., Dupouyet, S., and Bonin, G. (2002). Environmental Risks of Applying Sewage Sludge Compost to Vineyards. *J. Environ. Qual.* 31 (5), 1522–1527. doi:10.2134/jeq2002.1522

Larreur-Cayol, S., Bertron, A., and Escadeillas, G. (2011). Degradation of Cement-Based Materials by Various Organic Acids in Agro-Industrial Waste-Waters. *Cement Concrete Res.* 41 (8), 882–892. doi:10.1016/j.cemconres.2011.04.007

Lee, N. K., and Lee, H. K. (2016). Influence of the Slag Content on the Chloride and Sulfuric Acid Resistances of Alkali-Activated Fly Ash/slag Paste. *Cement and Concrete Composites* 72, 168–179. doi:10.1016/j.cemconcomp.2016.06.004

Lloyd, R. R., Provis, J. L., and van Deventer, J. S. (2012). Acid Resistance of Inorganic Polymer Binders. 1. Corrosion Rate. *Mater. structures* 45 (1-2), 1–14. doi:10.1617/s11527-011-9744-7

Longhi, M. A., Rodríguez, E. D., Walkley, B., Zhang, Z., and Kirchheim, A. P. (2020). Metakaolin-based Geopolymers: Relation between Formulation, Physicochemical Properties and Efflorescence Formation. *Composites B: Eng.* 182, 107671. doi:10.1016/j.compositesb.2019.107671

Ma, Y., Yang, X., Hu, J., Zhang, Z., and Wang, H. (2019). Accurate Determination of the "Time-Zero" of Autogenous Shrinkage in Alkali-Activated Fly Ash/slag System. *Composites Part B: Eng.* 177, 107367. doi:10.1016/j.compositesb.2019.107367

Mehta, A., and Siddique, R. (2017). Sulfuric Acid Resistance of Fly Ash Based Geopolymer concrete. *Construction Building Mater.* 146, 136–143. doi:10.1016/j.conbuildmat.2017.04.077

Messina, F., Ferone, C., Colangelo, F., Giuseppina, R., and Raffaele, C. (2018). Alkali Activated Waste Fly Ash as Sustainable Composite: Influence of Curing and Pozzolanic Admixtures on the Early-Age Physico-Mechanical Properties and Residual Strength after Exposure at Elevated Temperature. *Composites Part B: Eng.* 132, 161–169. doi:10.1016/j.compositesb.2017.08.012,

Muthu, M., and Santhanam, M. (2018). Effect of Reduced Graphene Oxide, Alumina and Silica Nanoparticles on the Deterioration Characteristics of Portland Cement Paste Exposed to Acidic Environment. *Cement and Concrete Composites* 91, 118–137. doi:10.1016/j.cemconcomp.2018.05.005

Nagadomi, H., Kitamura, T., Watanabe, M., and Sasaki, K. (2000). Simultaneous Removal of Chemical Oxygen Demand (COD), Phosphate, Nitrate and H2S in the Synthetic Sewage Wastewater Using Porous Ceramic Immobilized Photosynthetic Bacteria. *Biotechnol. Lett.* 22 (17), 1369–1374. doi:10.1023/a:1005688229783

Oueslati, O., and Duchesne, J. (2014). Resistance of Blended Cement Pastes Subjected to Organic Acids: Quantification of Anhydrous and Hydrated Phases. *Cement and Concrete Composites* 45, 89–101. doi:10.1016/j.cemconcomp.2013.09.007

Pacheco-Torgal, F., Abdollahnejad, Z., Camões, A. F., Jamshidi, M., and Ding, Y. (2012). Durability of Alkali-Activated Binders: A clear Advantage over Portland Cement or an Unproven Issue? *Construction Building Mater.* 30, 400–405. doi:10.1016/j.conbuildmat.2011.12.017

Parande, A. K., Ramsamy, P. L., Ethirajan, S., Rao, C. R. K., and Palanisamy, N. (2006). "Deterioration of Reinforced concrete in Sewer Environments," in Proceedings of the Institution of Civil Engineers - Municipal Engineer (Thomas Telford Ltd), 11–20. doi:10.1680/muen.2006.159.1.11159

Pavía, S., and Condren, E. (2008). Study of the Durability of OPC versus GGBS concrete on Exposure to Silage Effluent. *J. Mater. civil Eng.* 20 (4), 313–320. doi:10.1061/(asce)0899-1561(2008)20:4(313)

Provis, J. L., Palomo, A., and Shi, C. (2015). Advances in Understanding Alkali-Activated Materials. *Cement Concrete Res.* 78, 110–125. Part A. doi:10.1016/j.cemconres.2015.04.013

Quenea, K., Lamy, I., Winterton, P., Bermond, A., and Dumat, C. (2009). Interactions between Metals and Soil Organic Matter in Various Particle Size Fractions of Soil Contaminated with Waste Water. *Geoderma* 149 (3), 217–223. doi:10.1016/j.geoderma.2008.11.037

Ren, J., Guo, S.-Y., Su, J., Zhao, T.-J., Chen, J.-Z., and Zhang, S.-L. (2019). A Novel TiO2/Epoxy Resin Composited Geopolymer with Great Durability in Wetting-Drying and Phosphoric Acid Solution. *J. Clean. Prod.* 227, 849–860. doi:10.1016/j.jclepro.2019.04.203

Ren, J., Guo, S.-Y., Zhao, T.-J., Chen, J.-Z., Nicolas, R. S., and Zhang, L. (2020). Constructing a Novel Nano-TiO2/Epoxy Resin Composite and its Application in Alkali-Activated Slag/fly Ash Pastes. *Construction Building Mater.* 232, 117218. doi:10.1016/j.conbuildmat.2019.117218

Ren, J., Zhang, L., and Nicolas, R. S. (2021). Degradation of Alkali-Activated Slag and Fly Ash Mortars under Different Aggressive Acid Conditions. *J. Mater. Civil Eng.* 33 (7). doi:10.1061/(asce)mt.1943-5533.0003713

Ren, J., Zhang, L., and San Nicolas, R. (2020). Degradation of Alkali-Activated Slag/fly Ash Mortars under Different Aggressive Acid Conditions. *J. Mater. civil Eng.* 33 (7). doi:10.1061/(asce)mt.1943-5533.0003713

Ren, J., Zhang, L., and San Nicolas, R. (2020). Degradation Process of Alkali-Activated Slag/fly Ash and Portland Cement-Based Pastes Exposed to Phosphoric Acid. *Construction Building Mater.* 232, 117209. doi:10.1016/j.conbuildmat.2019.117209

Ren, J., Zhang, L., Walkley, B., Black, J. R., and San Nicolas, R. (2022). Degradation Resistance of Different Cementitious Materials to Phosphoric Acid Attack at Early Stage. *Cement Concrete Res.* 151, 106606. doi:10.1016/j.cemconres.2021.106606

Sánchez-Herrero, M. J., Fernández-Jiménez, A., and Palomo, A. (2017). C3S and C2S Hydration in the Presence of Na2CO3 and Na2SO4. *J. Am. Ceram. Soc.* 100 (7), 3188–3198. doi:10.1111/jace.14855

Sata, V., Sathonsaowaphak, A., and Chindaprasirt, P. (2012). Resistance of lignite Bottom Ash Geopolymer Mortar to Sulfate and Sulfuric Acid Attack. *Cement and Concrete Composites* 34 (5), 700–708. doi:10.1016/j.cemconcomp.2012.01.010

Scrivener, K., and De Belie, N. *Bacteriogenic Sulfuric Acid Attack of Cementitious Materials in Sewage Systems, Performance of Cement-Based Materials in Aggressive Aqueous Environments*. Springer2013, 305–318.

Song, X., Marosszeky, M., Brungs, M., and Munn, R. (2005). *Durability of Fly Ash Based Geopolymer concrete against Sulphuric Acid Attack, International Conference on Durability of Building Materials and Components*. Lyon [France]: Cement and Concrete Research, Elsevier, 17–20.

Suzzanna (2017). Cost of Urban Water Infrastructure Failure. Available at: https://membership.corrosion.com.au/blog/cost-of-urban-water-infrastructure-failure/ (Accessed February 22, 2017).

Sydney, R., Esfandi, E., and Surapaneni, S. (1996). Control concrete Sewer Corrosion via the crown spray Process. *Water Environ. Res.* 68 (3), 338–347. doi:10.2175/106143096x127785

Tang, S. W., Cai, X. H., He, Z., Zhou, W., Shao, H. Y., Li, Z. J., et al. (2016). The Review of Pore Structure Evaluation in Cementitious Materials by Electrical Methods. *Construction Building Mater.* 117, 273–284. doi:10.1016/j.conbuildmat.2016.05.037

Temuujin, J., Minjigmaa, A., Lee, M., Chen-Tan, N., and van Riessen, A. (2011). Characterisation of Class F Fly Ash Geopolymer Pastes Immersed in Acid and Alkaline Solutions. *Cement and Concrete Composites* 33 (10), 1086–1091. doi:10.1016/j.cemconcomp.2011.08.008

van Deventer, J. S. J., San Nicolas, R., Ismail, I., Bernal, S. A., Brice, D. G., and Provis, J. L. (2015). Microstructure and Durability of Alkali-Activated Materials

as Key Parameters for Standardization. *J. Sust. Cement-Based Mater.* 4 (2), 116–128. doi:10.1080/21650373.2014.979265

Varga, C., Alonso, M. M., Mejía de Gutierrez, R., Mejía, J., and Puertas, F. (2015). Decalcification of Alkali-Activated Slag Pastes. Effect of the Chemical Composition of the Slag. *Mater. Struct.* 48 (3), 541–555. doi:10.1617/s11527-014-0422-4

Xiao, J., Long, X., Qu, W., Li, L., Jiang, H., and Zhong, Z. (2022). Influence of Sulfuric Acid Corrosion on concrete Stress-Strain Relationship under Uniaxial Compression. *Measurement* 187, 110318. doi:10.1016/j.measurement.2021.110318

Xiao, J., Xu, Z., Murong, Y., Wang, L., Lei, B., Chu, L., et al. (2022). Effect of Chemical Composition of Fine Aggregate on the Frictional Behavior of Concrete–Soil Interface under Sulfuric Acid Environment. *Fractal and Fractional* 6 (1), 22. doi:10.3390/fractalfract6010022(

Xie, J., Wang, J., Rao, R., Wang, C., and Fang, C. (2019). Effects of Combined Usage of GGBS and Fly Ash on Workability and Mechanical Properties of Alkali Activated Geopolymer concrete with Recycled Aggregate. *Composites Part B: Eng.* 164, 179–190. doi:10.1016/j.compositesb.2018.11.067

Yan, S., He, P., Jia, D., Wang, J., Duan, X., Yang, Z., et al. (2017). Effects of High-Temperature Heat Treatment on the Microstructure and Mechanical Performance of Hybrid Cf-SiCf-(Al2O3p) Reinforced Geopolymer Composites. *Composites Part B: Eng.* 114, 289–298. doi:10.1016/j.compositesb.2017.02.011

Yang, G., Fan, M., and Zhang, G. (2014). Emerging Contaminants in Surface Waters in China-a Short Review. *Environ. Res. Lett.* 9 (7), 074018. doi:10.1088/1748-9326/9/7/074018

Zivica, V., and Bajza, A. (2002). Acidic Attack of Cement-Based Materials-A Review Part 2. Factors of Rate of Acidic Attack and Protective Measures. *Construction building Mater.* 16 (4), 215–222. doi:10.1016/s0950-0618(02)00011-9

Conflict of Interest: The authors declare that the research was conducted in the absence of any commercial or financial relationships that could be construed as a potential conflict of interest.

Publisher's Note: All claims expressed in this article are solely those of the authors and do not necessarily represent those of their affiliated organizations, or those of the publisher, the editors, and the reviewers. Any product that may be evaluated in this article, or claim that may be made by its manufacturer, is not guaranteed or endorsed by the publisher.